Desalination and Water Treatment
www.deswater.com
doi: 10.5004/dwt.2018.22999

133 (2018) 45–54
November

Application of MFI-UF fouling index with NOM fouling under various operating conditions

Mohammad T. Alresheedi*, Onita D. Basu

Department of Civil and Environmental Engineering, Carleton University, 1125 Colonel By Drive, Ottawa, ON, K1S 5B6, Canada, Tel. 1-613-520-2600; emails: mohammadalresheedi@cmail.carleton.ca (M.T. Alresheedi), Onita.basu@carleton.ca (O.D. Basu)

Received 7 March 2018; Accepted 24 August 2018

ABSTRACT

Fouling research with polymeric membranes has demonstrated that various natural organic matter (NOM) fractions contribute differentially to membrane fouling behavior. However, limited studies exist analyzing the sensitivity of the MFI-UF to be used as a tool to differentiate NOM fouling components. The results here indicate that MFI-UF is a suitable tool for assessing NOM fouling. Specifically, NOM fouling potential was in the order of organic proteins (as BSA), polymers (alginate), and humic acid, respectively. Further, a mixed solution containing BSA, alginate and humic acid fouled similarly to the BSA solution indicating the high fouling potential of organic proteins in membrane systems. The MFI-UF value was found to increase by > 30% with increasing pressure (1–3 bar) and decreasing temperature (35°C–5°C). The filtered water volume was found to correlate with the MFI-UF values indicating the dependency of the method on testing conditions. Incorporating water viscosity and pressure values against normalized conditions (20°C and 2 bar) with the standard MFI-UF equation was found to be useful to estimate MFI-UF values at variable operating conditions, thus, enhances the potential application range of MFI-UF as a fouling index for NOM.

Keywords: MFI-UF; Humic acid; BSA; Sodium alginate; Temperature

1. Introduction

Ultrafiltration (UF) is considered a promising process for drinking water production because of its easy automation, compactness, and high removal rate of various water contaminants [1]. However, one of the main challenges in membrane processes is fouling which decreases membrane efficiency in terms of flux, increases pressure requirements and cleaning frequency, and ultimately decreases the lifetime of the membrane unit [2]. Previous studies on membrane fouling have provided valuable insights on the major foulants during the filtration of natural waters. This includes natural organic matter (NOM), inorganic substances, particulate/colloids matter, and microbiological compounds [3,4]. Among these foulants, membrane fouling by NOM is the major concern in membrane processes to treat surface water [4]. The major NOM fractions that have been linked to membrane fouling were identified as humic acids, proteins, and polysaccharide like substances [5–7]. Therefore, prevention and control of NOM fouling are essential for successful operation of membrane systems.

Over the past decades, researchers have focused their effort to develop fouling prediction methods such as the silt density index (SDI) and modified fouling index (MFI), to assess the fouling potential of membrane feed with a goal of reducing the fouling problem. These methods are indirect estimate of fouling potential making use of microfiltration (MF) filters with pores of 0.45 μm. The simplicity of these tests has led to their popularity; however, there are growing doubts about the accuracy of these tests for fouling prediction. Membranes manufacturers are frequently questioned that the filtered water does not meet the SDI/MFI values

* Corresponding author.

reported by the manufacturer nor the treatment requirement [8]. These observations could be attributed to the lack of agreement between fouling indices testing conditions and membrane systems. In fact, it has been proven that particles smaller than 0.45 μm contribute to membrane fouling [9,10]. Therefore, Boerlage et al. [10] developed the MFI-UF, making use of UF membranes to count for particles <0.45 μm. The MFI–UF has been tested for seawater and used at constant pressure and constant flux [10,11]. Feed water having an MFI-UF < 3,000 s/L^2 is equivalent to SDI < 3 %/min, which is acceptable for membrane feed [10]. The utilization of the MFI-UF for assessing the fouling propensity has been carried out in recent studies [12–16]. For example, Rodriguez et al. [12] and Jeong et al. [13] used the MFI-UF to assess particulate and biofouling potential for RO systems. Moreover, MFI-UF was applied to assess fouling potential of different species of bloom forming algae in marine and freshwater sources [14]. Other studies [15,16], investigated the influence of inorganic silica and calcium colloids on the MFI-UF fouling index for seawater RO systems. The MFI-UF showed promising results with regards to assessing fouling, however, to date, the applicability of the MFI-UF testing to predict NOM fouling for low pressure membranes has received little attention.

The standardized MFI-UF test is performed under a constant pressure of 2 bar and temperature of 20°C. However, operating pressure and water temperature change seasonally and over filtration cycles in membrane systems, thus developing a model away from standard conditions may extend its useful applicability. Moreover, to date, the ability of the MFI-UF to predict NOM fouling under changes of membrane process conditions has received little attention, which is necessary for the successful implementation of MFI-UF for NOM fouling prediction. Therefore, the objectives of this research are to evaluate the MFI-UF method as a tool to predict fouling of various NOM fractions commonly found in surface water sources. Further to assess the MFI-UF method under a range of pressure and temperature conditions in low pressure membrane systems and to propose an empirical model that can be used to extend its useful application range for fouling studies.

2. Materials and methods

2.1. Experimental setup and approach

The MFI-UF setup consisted of a digital gear pump (Cole Parmer: Drive No. 75211-30, Head No. 07003-04); a ball valve (Cole Parmer No. 01377-18); a pressure relief valve (Aquatrol No. 3ETU4), and a pressure regulator with gauge (Veolia No. LA512). PAN UF, hollow fiber, inside-out membrane module (Pall Corp., Canada) was used and its characteristics are presented in Table 1. This UF membrane was proposed by Boerlage et al. [10]. High-capacity precision top loading balance (Adam Equipment NBL8201e) to measure the permeate volume. A schematic representation of the MFI-UF setup is shown in Fig. 1.

The MFI-UF (constant pressure) was performed according to method described by Boerlage et al. [10]. Feed water was filtered through the UF membrane under dead-end mode, constant pressure while monitoring flux decline during the test. Permeate was collected in a tank set on

Table 1
MFI-UF membranes characteristics

Membrane type	UF – 13 kDa
Membrane materials	PAN hollow fiber
Configuration	Inside-out
Fiber ID	0.8 mm
Fiber OD	1.4 mm
Number of fiber	400
Membrane area	0.2 m^2
Module length	347 mm
Module diameter	42 mm

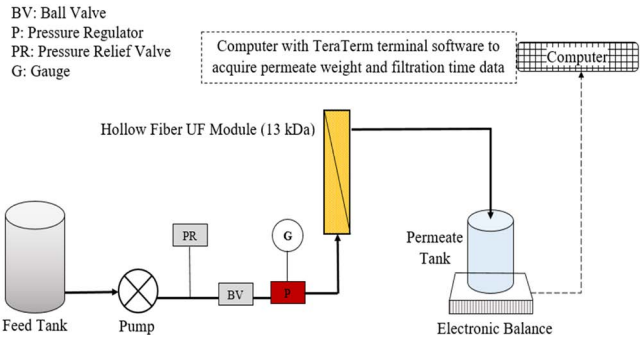

Fig. 1. A schematic representation of the MFI-UF setup.

the electronic balance which has an RS 232 interface with a computer in order to acquire permeate weight and filtration time data from the balance. Data were recorded every 1 min and imported into MS Excel spread sheet with data terminal software (TeraTerm). The MFI-UF was then calculated using Eq. (1) [10].

$$\frac{t}{V} = \frac{\mu R_m}{\Delta P A} + \left(\frac{\mu C_b \alpha}{2 \Delta P A^2}\right) V = \frac{\mu R_m}{\Delta P A} + \text{MFI} - \text{UF}_{\text{exp}}\left(V\right) \quad (1)$$

which can be rewritten as

$$\text{MFI} - \text{UF}_{\text{exp}} = \frac{d\left(\frac{t}{V}\right)}{dV} \quad (2)$$

where t is the filtration time (s); V is permeate produced (m^3); ΔP is the pressure (bar); μ is the viscosity of water (kg/m s); A is the membrane area (m^2); R_m is the membrane resistance (m^{-1}); α is the specific cake resistance (m/kg); and C_b is the bulk concentration (kg/m^3). The MFI-UF$_{\text{experimental}}$ (MFI-UF$_{\text{exp}}$) represents the slope of the linear portion of the t/V versus V in Eq. (2) [10]. The slope of two data points from the t/V and V measurements was calculated overtime and used to graph the MFI-UF as a function of filtration time [10,17]. Boerlage study [10] showed that the MFI-UF value increases sharply with time during first few hours of filtration due to pore blocking then stabilizes afterwards (i.e., remains unchanged for several hours). The stabilization of the MFI-UF value

was believed to be due to the occurrence of cake filtration in which the rate of increase in the filtered water volume remains constant with time. Thus, in this study, the final MFI-UF was determined by averaging the MFI-UF data in the most stable region of the MFI-UF graph [10]. To examine the effect of testing conditions on the MFI-UF measurements, experiments were carried out under various pressure and temperature conditions. The operating pressure was varied between 1, 2, and 3 bar (15, 30, and 45 psi) whereas water temperature was varied between 5°C, 10°C, 20°C, 30°C, and 35°C.

The UF membrane was cleaned after each MFI-UF experiment. The membrane was first rinsed with DI water for approximately 30 min followed by chemical cleaning using sodium hypochlorite (200 ppm), which was recirculated for 60 min at ambient temperature followed by citric acid clean (1%). Clean water flux was measured before any experiment and calculated using Eq. (3) [18] corrected to temperature of 20°C and pressure of 2 bar (recommended by the manufacture). This was important to ensure good stability of the UF membrane before any experiment.

$$J_{20^\circ C} = J_m (1.03)^{T_{20^\circ C} - T_m} \quad (3)$$

2.2. Feed solutions

Four different synthetic feed water solutions used in this study. Humic acids (2.5 mgC/L), a protein (bovine serum albumin, BSA, 2.5 mgC/L), a polysaccharide (sodium alginate, 2.5 mgC/L), and a mixture of the three NOM models (0.83 mgC/L/each NOM model, total of 2.5 mgC/L), were used as model NOM foulants. These NOM models are commonly found in surface water and can significantly contribute to membrane fouling [7,19]. All model substances were purchased from Sigma Aldrich, Canada. A moderate hardness and alkalinity of 75 mg/L calcium carbonate ($CaCO_3$) and a low level of turbidity (5 NTU) as kaolin clay particles were included in the synthetic water matric to represent the more complex conditions of a surface water source. Previous research on fouling during surface water treatment have reported that calcium will cause the NOM particles to be less negative due to double layer compression and reduction of the electrostatic repulsion forces between particles and membrane surface, thus, increasing NOM fouling rate [5,20]. In addition, the presence of kaolin clay particles during filtration was reported to act as an adsorbent of NOM, thus, increasing NOM adsorption onto the membrane surface and consequently resulting in high flux decline [20]. Therefore, in this study, it was necessary to examine NOM-calcium-particles interactions in water during MFI-UF testing. This is of particular importance because the raw water characteristics may vary significantly with respect to the NOM, calcium, and particle concentrations, thus, impacting fouling estimation.

Feed solutions were prepared using DI water and were mixed using a magnetic stirrer 1-d prior any experiment to ensure that materials were dissolved completely. Feed water was continuously mixed using a dual speed mixer to ensure homogeneous water conditions throughout the experiment. The feed tank was insulated to maintain constant temperature throughout the testing period. An immersion heater (Cole Parmer) and a compact chiller (LM series, Polyscience) were used to adjust the water temperature as required. Temperature and pH were monitored continuously using HACH (cat.no. 58258-00) HQd Field Case equipment. The pH of the feed was maintained around 7.5.

2.3. Analysis

2.3.1. Molecular weight fractionation of NOM

The molecular weight distribution of the feed solutions, which are comprised of the respective NOM components, kaolin clay, and calcium, was determined by UF fractionation method using a 400 mL UF stirred cell (model 8400, Amicon Inc., Canada) and five hydrophilic regenerated cellulose membranes (Millipore, Bradford MA) with different molecular weight cut-offs (MWCOs) of 1,000, 5,000, 10,000, 30,000, and 100,000 Da. 2 L of feed water solutions were prepared for the fractionation. The fractionation was performed sequentially by passing 400 mL of sample through the membrane with the highest MWCO to that with the lowest MWCO. Samples from permeate and retentate of particular membrane were collected and total organic carbon (TOC) was analyzed using Tekmar Dohrmann, Phoenix 8000 TOC analyzer. Excess permeate produced by each fractionation step was used as the feed to the next membrane with a lesser MWCO. The UF fractionation method used in this study is described in detail by [21,22]. The TOC concentration of a particular molecular weight fraction was calculated by subtracting the TOC concentration of the filtrate from one membrane from the TOC concentration of the filtrate from the membrane of the next larger nominal MWCO. After fractionation experiments, membranes were rinsed with Milli-Q water for 60 min changing the water three times (i.e., every 20 min) and stored in 10% by volume ethanol/water solution and kept in refrigerator at 4°C for later use. Prior to use, the membranes were rinsed several times after which Milli-Q water was allowed to filtered through them for three times.

2.3.2. MFI-UF data analysis

One-way ANOVA (using the *F*-test) on the data collected to determine the significance of the MFI-UF measured at different pressure and temperature conditions. The mean difference between conditions was considered to be significant at a *p*-value of ≤ 0.05. Post-ANOVA test (Tukey HSD test) was then performed to determine pair-wise comparisons between the various testing conditions.

To differentiate between pore blocking and cake filtration mechanisms during the MFI-UF testing, the combined model proposed by Ho and Zydney [23] was used to analyze the filtration data. Four major fouling mechanisms are described as complete pore blocking ($n = 2$), standard blocking ($n = 1.5$), intermediate blocking ($n = 1$), and cake filtration ($n = 0$). A generalized equation describing the mechanisms is shown in Eq. (4).

$$\frac{d^2t}{dV^2} = k\left(\frac{dt}{dV}\right)^n \quad (4)$$

which can be rewritten as

$$\log\left(\frac{d^2t}{dV^2}\right) = \log k + n\log\left(\frac{dt}{dV}\right) \quad (5)$$

in which t is time (s), V is water volume (L), and k is blocking law filtration coefficient (units vary depending on n), and n is blocking law filtration exponent (unitless).

2.3.3. Modeling of the MFI-UF

Operating pressure and water temperature change seasonally and over filtration cycle time periods in membrane systems, thus, it may not be practical to alter an MFI-UF setup for different operating pressures or water temperatures. In this study, the MFI-UF_{exp} calculated from the slope of the linear portion of the t/V versus V graphs (i.e., Eq. (2)) was normalized to (MFI-UF_{nor}) by including pressure and viscosity correction terms as shown in Eq. (6). This was important to determine the ability of the MFI-UF to predict fouling conditions away from the standard reference conditions. The normalized model is derived from the MFI model, ASTM method [24]. In addition, a general linear regression modeling (GLM) (Eq. (7)), was used to estimate the predicted MFI-UF value (MFI-UF_{pr}) at different conditions. The MFI-UF_{pr} was utilized to establish the influence of the operating pressure and water temperature on the final MFI-UF values. The MFI-UF_{exp} was then compared with the MFI-UF_{nor} and MFI-UF_{pr}.

$$\text{MFI}-\text{UF}_{nor} = \frac{\mu_{20^\circ C}}{\mu_T} \times \frac{P}{P_0} \times \text{MFI}-\text{UF}_{exp} \quad (6)$$

$$\text{MFI-UF}_{pr} = \beta_0 + \beta_1\,\text{Pressure} + \beta_2\,\text{Temperature} \quad (7)$$

where μ_T and P are the water viscosity, operating pressure respectively. $\mu_{20^\circ C}$ and P_0 are included to normalize the MFI-UF values to the standard reference conditions of pressure and temperature (i.e., 2 bar and 20°C). β_0, β_1, and β_2 are the intercept and regression coefficients related to the effect of pressure and temperature, respectively.

3. Results and discussion

3.1. Molecular weight distribution of feed solutions

The molecular weight distribution analysis of feed solutions (refer to Fig. 2) indicates that the majority of the particles in the feed water are greater than 30 kDa, thus a higher percentage of particles (>70%) is expected to be retained by the MFI UF 13 kDa membrane. Feed solutions containing BSA and NOM mixture showed higher percentage of particles in the range of > 30 kDa, thus, it is expected to cause pore blocking and have a higher MFI-UF value than the other organic fractions. The MW distribution of the humic acid and alginate feed solutions is approximately similar which indicates that the differences in fouling would be highly influenced by their chemical and material properties versus size alone. However, all four model solutions are expected to foul the membranes by cake formation, pore blockage, or a combination of both as commonly occurs in a UF membrane process.

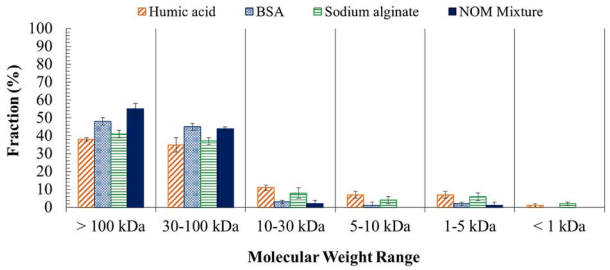

Fig. 2. Molecular weight distribution of feed water solutions.

3.2. Effect of variation of operating pressure and water temperature on the MFI-UF measurement to predict NOM fouling

3.2.1. MFI-UF measurement under variable operating pressure

In order to determine the MFI-UF values for each testing condition, the slope of two data points from the t/V and V measurements is calculated overtime and used to graph the MFI-UF as a function of filtration time [10,17]. Fig. 3 is an example of the MFI-UF curves as a function of time under different operating pressures. It can be clearly seen that the MFI-UF graph in Figs. 3(a) and (c) is divided into two regions: at the beginning of filtration (the first region), the MFI-UF increases sharply during the first 1–1.5 h of filtration. This sharp increase in the MFI-UF value is due to pore blocking as indicated by Boerlage et al. [10]. The blocking law exponent (n) values were determined for each testing condition by plotting the log d^2t/dV^2 versus log dt/dV (Figs. 3(b) and (d) as an example) which range from 1.431 to 1.833 and from 1.772 to 2.040 for 1 and 3 bar, respectively. The n values are very close to 1.5–2 indicating the occurrence of standard and complete pore blocking mechanism within the first 1–1.5 h of filtration. After 2.5–3 h of filtration, the MFI-UF value rate change slows and then stabilizes for the duration of the test. The stabilization of the MFI-UF value is related to the occurrence of cake filtration (the second region) at which the increase in the accumulated filtered water volume remains constant with time [10]. The n values for the cake filtration region (refer to Figs. 3(b) and (d) as an example) are close to 0 which range from 0.014 to 0.082 and from 0.043 to 0.120 for 1 and 3 bar, respectively. The final MFI-UF values are determined by taking the average of MFI-UF data in the most stable region in the MFI-UF curve. The MFI-UF was found to stabilize (i.e., minimum to no change) after 3–6 h of filtration.

The MFI-UF_{exp} values (Fig. 4) increased with increasing operating pressure. At higher operating pressure, more particles were forced towards the membrane forming a denser cake layer with lower porosity and higher resistance [17], hence, higher MFI-UF value. Moreover, the increase in filtration pressure led to an increase in flux which may cause compression of the cake layer and lead to higher MFI-UF value. The results from a one-way ANOVA (Table S1(a)) indicate that the MFI-UF_{exp} values estimated at different pressure conditions were significant ($p < 0.05$). Post-ANOVA analysis illustrates that the difference between all three pressure categories were also significant (p-values < 0.05). This indicates that MFI-UF_{exp} testing is dependent on the pressure condition

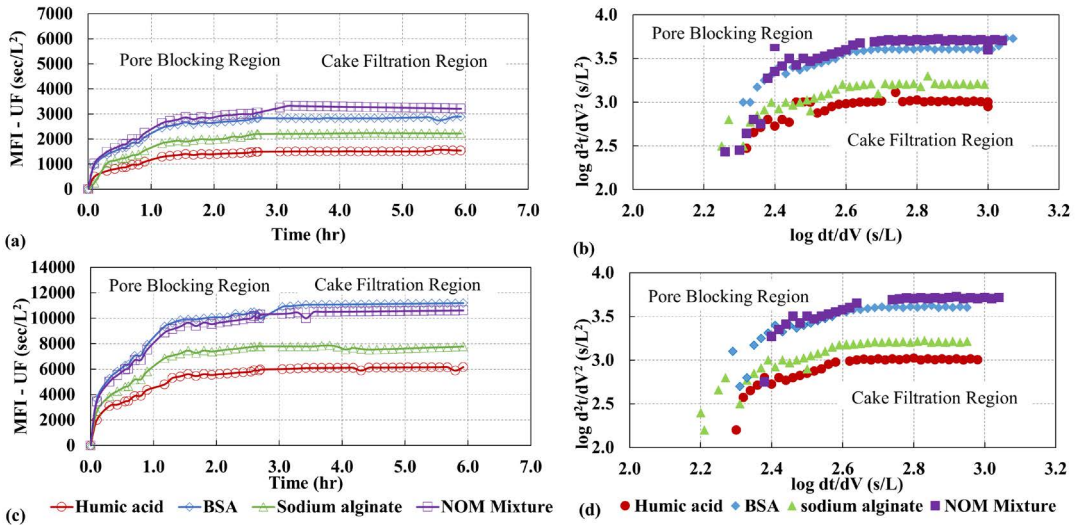

Fig. 3. Example of MFI-UF and filtration mechanism graphs for the NOM fractions at different pressure (T = 20°C). (a) MFI-UF versus time (P = 1 bar); (b) d^2t/dV^2 versus dt/dV curves (P = 1 bar); (c) MFI-UF versus time (P = 3 bar); and (d) d^2t/dV^2 versus dt/dV curves (P = 3 bar).

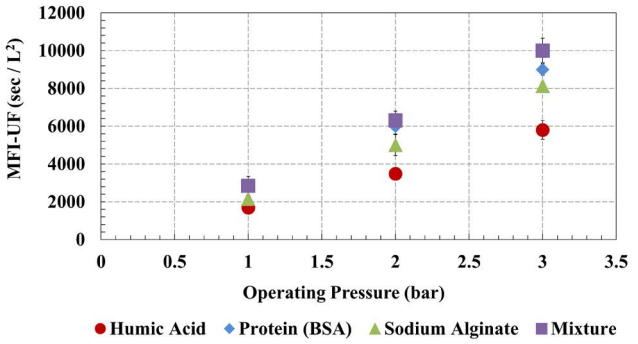

Fig. 4. MFI-UF_{exp} measured for various NOM fractions at different operating pressure (T = 20°C).

and that the fouling rate of the membrane will change as pressure changes in the system; highlighting the importance of assessing fouling index values at both a reference standard condition to compare between general water system but also at operational conditions to increase the predictive power and analysis of the fouling tests.

Fouling potential of different feed water types predicted by the MFI-UF (constant pressure) was in the order of NOM mixture, BSA (protein), sodium alginate, and humic acid, respectively. The differences between fouling among the four types of NOM could be attributed to the molecular weight distribution (refer to Fig. 2). Feed water solutions containing BSA and NOM mixture have higher components with molecular weight in the range of 30–100 and >100 kDa which was much larger than the MWCO of the UF membrane (13 kDa) and may therefore resulted in more pore blocking leading to higher fouling, thus, higher MFI-UF value compared with sodium alginate and humic acid. These results are also analogous to those by [7,19] using polymeric MF and UF membranes for fouling experiments, in which humic acid had lower fouling rate compared with BSA and alginate under constant pressure filtration experiments. The MFI-UF was able to predict this fouling order which highlights the applicability of the MFI-UF for NOM fouling prediction for low pressure membranes. The NOM mixture resulted in the highest MFI-UF value. This is attributed to the complete pore blocking mechanism of the NOM mixture (n ranges between 1.833 and 2.040), refer to Figs. 3(b) and (d), thus, higher final MFI-UF value compared with humic acid, BSA, and alginate alone. This can be supported by molecular weight fractionation (refer to Fig. 2), in which the NOM mixture solution has higher percentage in the size range of >30 kDa, thus, it is expected to cause complete pore blocking to the 13 kDa UF membrane and higher MFI-UF.

3.2.2. MFI-UF measurement under variable water temperature

Fig. 5 is an example of the MFI-UF curves as a function of time under different temperature conditions. It can be clearly seen that the MFI-UF graph in Figs. 5(a) and (c) is divided into two regions: at the beginning of filtration (the first region), the MFI-UF increases sharply due to pore blocking. The blocking law exponent (n) values during the first 1–1.5 h of filtration (refer to Figs. 5(b) and (d) as an example) range from 1.800 to 2.060 and from 1.332 to 1.665 for 5°C and 35°C respectively. The n values are very close to 2 indicating the occurrence of pore blocking mechanism. After 2.5–3 h of filtration, the MFI-UF value rate change slows and then stabilizes for the duration of the test indicating the occurrence of cake filtration (the second region) [10]. The n values for the cake filtration region (refer to Figs. 5(b) and (d) as an example) range from 0.027 to 0.130 and from 0.011 to 0.066 for 5°C and 35°C, respectively. The final MFI-UF values are determined by taking the average of MFI-UF data in the most stable region in the MFI-UF curve. The MFI-UF was found to stabilize (i.e., minimum to no change) after 3–6 h of filtration. The MFI-UF graphs at low water temperature (5°C) follow similar trend as MFI-UF graphs at high pressure (3 bar) and vice versa.

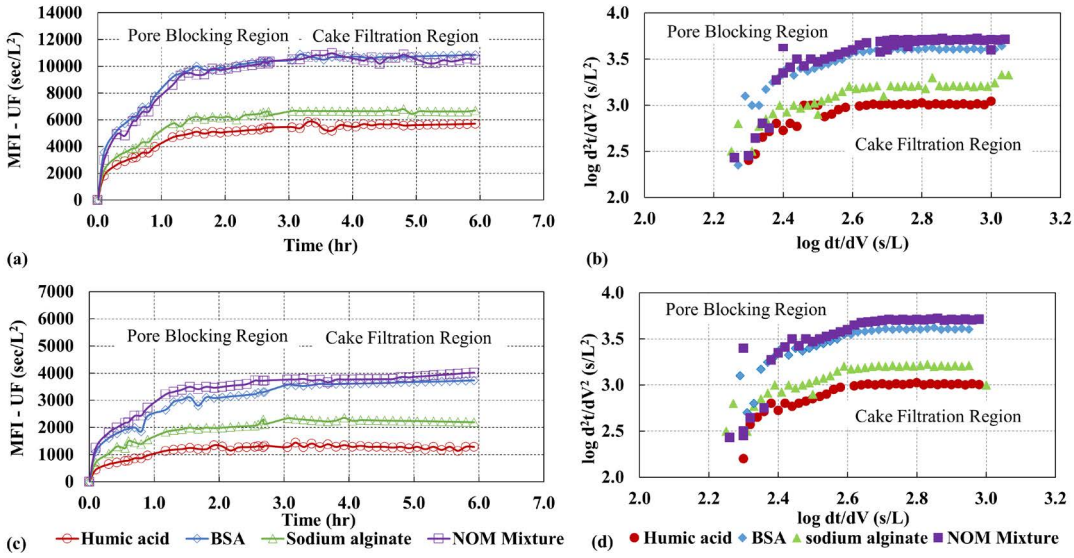

Fig. 5. Example of MFI-UF and filtration mechanism graphs for the NOM fractions at different temperature (P = 1 bar). (a) MFI-UF versus time (T = 5°C); (b) d^2t/dV^2 versus dt/dV curves (T = 5°C); (c) MFI-UF versus time (T = 35°C); and (d) d^2t/dV^2 versus dt/dV curves (T = 35°C).

The MFI-UF$_{exp}$ values (Fig. 6) decreased with increasing water temperature for all NOM solutions. NOM in cold water temperatures appears to have higher fouling potential compared with that at warmer temperatures. This could be a critical issue in predicting NOM fouling specifically in regions where there is a large seasonal variation in water temperature, as in North America and some parts of Europe. The effect of water temperature on membrane flux was reported to be 3% per 1°C changes in water temperature [18]. Under constant pressure, the variation in water temperature affected the flux through the UF membrane and ultimately impacted the final MFI-UF measurements. In addition, the decrease in water temperature may cause shrinkage to the cake layer leading to a formation of denser cake with high specific cake resistance, thus, higher MFI-UF [25]. The fouling potential order of NOM is comparable with that at different pressure conditions.

ANOVA (Table S1(b)) analysis shows that the MFI-UF$_{exp}$ values estimated at different temperature conditions were significant (p < 0.05). Post-ANOVA test illustrates that the difference within groups (e.g., mean of humic acid MFI-UF at 5°C vs 30°C) was also significant (p-values < 0.05), demonstrating that the MFI-UF$_{exp}$ testing is dependent on the temperature condition.

3.2.3. MFI-UF surface plots and TOC rejection

The MFI-UF$_{pr}$, using GLM (Eq. (7)), was used to establish the influence of the operating pressure and water temperature on the final MFI-UF values. GLM results indicated that both parameters were of significance (Table S1(c)). Eqs. (7A)–(D) are the GLM models for different NOM fractions. It should be noted that the β values are the standardized regression coefficients (Table S1(c)) and thus, the relative importance of pressure and temperature can be compared regardless of their units. From Eqs. (7A)–(D), it can be clearly seen that for all model NOM, the MFI-UF value increases by 0.652–0.755

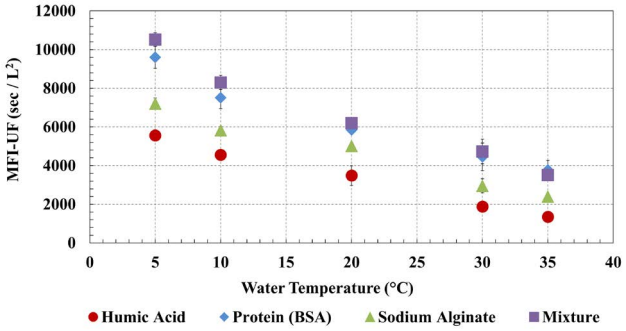

Fig. 6. MFI-UF$_{exp}$ measured for various NOM fractions at different water temperature (P = 2 bar).

units with a unit increase in pressure, holding temperature as a constant. In contrast, the standardized regression coefficient for temperature indicates that for a unit increase in temperature, the MFI-UF decreases by 0.609–0.691 units, holding pressure as a constant. From these models, it is clear that the pressure and temperature both influence the MFI-UF value but in opposing directions.

$$\text{MFI-UF}_{pr} = (\beta_0 + \beta_1 \text{ Pressure} + \beta_2 \text{ Temperature}) \quad (7)$$

$$\text{MFI-UF}_{pr} \text{ (Humic)} = (1{,}589 + 0.652P - 0.623T) \quad (7A)$$

$$\text{MFI-UF}_{pr} \text{ (Protein)} = (3{,}352 + 0.721P - 0.691T) \quad (7B)$$

$$\text{MFI-UF}_{pr} \text{ (Alginate)} = (1{,}189 + 0.755P - 0.609T) \quad (7C)$$

$$\text{MFI-UF}_{pr} \text{ (Mixture)} = (2{,}599 + 0.739P - 0.653T) \quad (7D)$$

Fig. 7 presents 3D surface plots of the MFI-UF as a function of pressure and temperature. The plots illustrate that

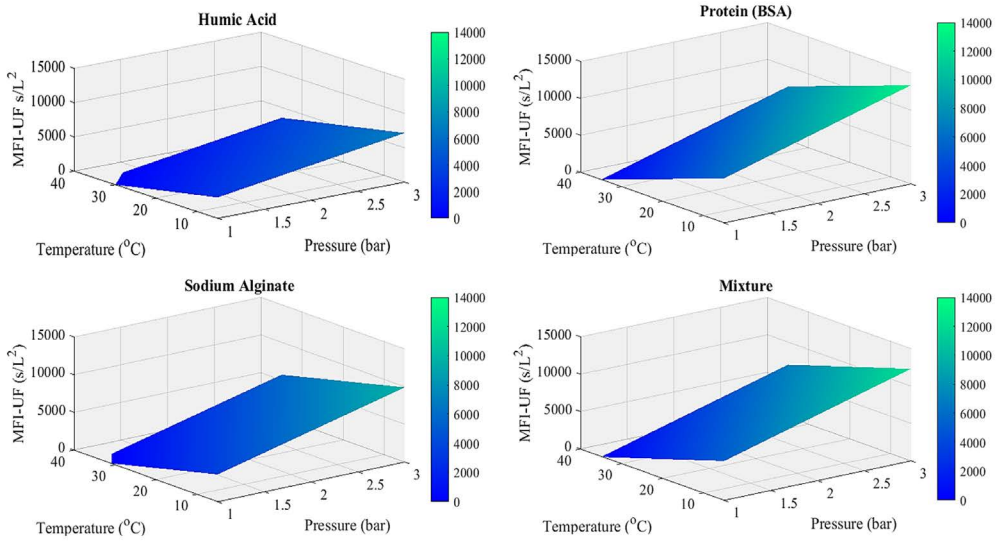

Fig. 7. 3D surface plots of the MFI-UF as a function of pressure and temperature.

the MFI-UF value increases with increasing pressure and decreasing temperature. According to Darcy's law, membrane resistance is dependent on both the pressure and water viscosity. The increase in MFI-UF with pressure increase or temperature decrease could be attributed to resistance increase of the fouling layer, thus, higher MFI-UF values. Proteins (BSA) were found to be particularly sensitivity to increases in pressure, as was the NOM mixture, however this is attributed to the protein component in the mixture as a dominant foulant.

Fig. 8 illustrates the TOC rejection by the 13 kDa UF membrane versus the MFI-UF fouling index. The TOC measurements were utilized to assess the MFI-UF fouling prediction and to determine any direct correlations between the MFI-UF value determined and the TOC rejected by the UF membrane. This is particularly important as there is no research that has used the TOC measurement as a method of assessing the predictability of the MFI-UF testing.

The TOC rejection of different feed solutions was found to decrease with increasing temperature. At lower temperature (5°C), >60% of TOC was rejected by the UF membrane for all model solutions whereas <45% of TOC was rejected at 35°C. Under all temperature conditions, the highest rejection was for BSA and NOM mixture whereas lower rejection for humic acids and alginate. Therefore, the increase in the MFI-UF value at low temperature was related to the high NOM rejection by the UF membrane whereas at high temperature, NOM was passing through the UF membrane to the filtrate side, thus, lower fouling and MFI-UF value.

3.3. Modeling of MFI-UF measurements ($MFI\text{-}UF_{exp}$, $MFI\text{-}UF_{nor}$, and $MFI\text{-}UF_{pr}$)

Operating pressure and water temperature change seasonally and over filtration cycle time periods in membrane systems, thus the current value of the MFI-UF test performed at the standard conditions of 2 bar and 20°C, while useful for comparing across studies, can overestimate or underestimate the fouling potential of NOM in site specific challenges.

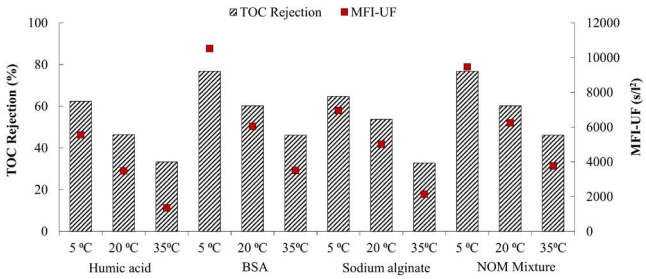

Fig. 8. MFI-UF and TOC rejection with water temperature conditions (P = 2 bar).

An empirical based model that can calculate MFI-UF values at nonstandard operating conditions is proposed to help extend its useful applicate range in terms of NOM fouling assessments.

The MFI-UF value is calculated from relationship between the inverse of the flow rate (t/V) and the permeate volume (V). The observed changes in the MFI-UF value at different pressure and temperature conditions could be related to the changes in filtration characteristics (e.g., flow, viscosity, etc.) and/or fouling layer properties. Therefore, the next step was to plot the $MFI\text{-}UF_{exp}$ values versus the final filtered water volume and determine if the filtered water volume reflects the fouling conditions observed during testing. Ideally, higher filtered water volume indicates lower MFI-UF value and vice versa. Fig. 9 presents the filtered water volume as a function of $MFI\text{-}UF_{exp}$ for different NOM solutions. Overall, it can be clearly seen that the water volume decreases with increasing $MFI\text{-}UF_{exp}$ value (R^2 between 0.68 and 0.78) which indicates that both pressure and temperature conditions heavily influence results. The changes in the final filtered water volume are an indicator of the changes in filtration characteristics of NOM water at the different conditions examined.

As both parameters (pressure and temperature) were found to be statistically significant, the next step was to use

the model that incorporates water temperature and operating pressure, MFI-UF$_{nor}$ (Eq. (6)) to assess the ability of the MFI-UF to predict NOM fouling conditions away from the standard reference conditions.

$$\text{MFI}-\text{UF}_{nor} = \frac{\mu_{20^\circ\text{C}}}{\mu_T} \times \frac{P}{P_0} \times \text{MFI}-\text{UF}_{exp} \quad (6)$$

Fig. 10 presents a comparison between the MFI-UF$_{exp}$ (Eq. (2)) MFI-UF$_{nor,}$ (Eq. (6)), and the MFI-UF$_{pr}$ (GLM, Eq. (7)). The MFI-UF$_{nor}$ values in Fig. 10 match the MFI-UF$_{exp}$ at the referenced testing conditions (i.e., 2 bar, 20°C) but deviate by 10%–15% at other nonreferenced conditions. Therefore, the observed increase or decrease in the MFI-UF$_{exp}$ values measured at different conditions was mainly attributed to the fouling tendency of water at specific filtration condition. Thus, the MFI-UF$_{exp}$ values measured at standard conditions

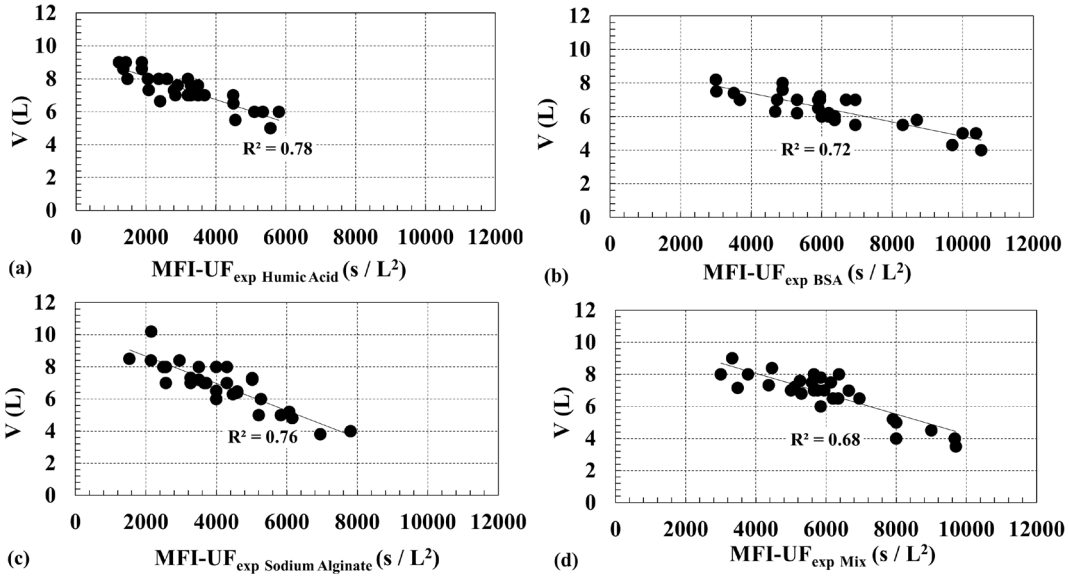

Fig. 9. MFI-UF as a function of filtered water volume for the four different synthetic solutions: (a) humic acid, (b) BSA, (c) sodium alginate, and (d) NOM mixture.

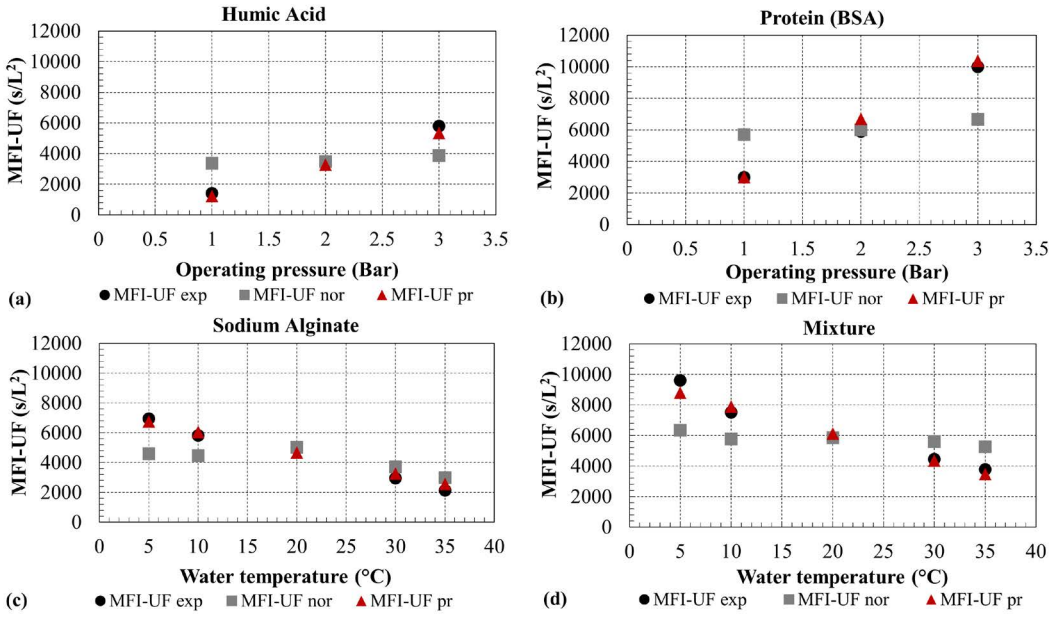

Fig. 10. MFI-UF$_{exp}$, versus MFI-UF$_{nor}$ versus MFI-UF$_{pr}$ for different model solutions.

can be altered to actual filtration conditions by adjusting the pressure and viscosity terms in the MFI-UF equation.

Thus, from these results, instead of having to design an MFI-UF test for the changes in temperature and pressure, the GLM Eqs. (7A)–(D) can be used as preliminary assessment of NOM fouling potential under changes in operational conditions. Future research should investigate the effect of water chemistry (i.e., pH, ionic strength, etc.) on the MFI-UF, as well as advancing the use of MFI-UF as a fouling prediction method for full scale membrane systems.

4. Conclusions

The presence of NOM in water poses major implications for membrane processes to maintain operational performance. This research investigated the application of the MFI-UF method to predict fouling of various NOM fractions under changes in pressure and temperature. The following points summarize the outcomes of this research:

- The NOM fouling potential order predicted by the MFI-UF_{exp} was NOM mixture, BSA, alginate, humic acid, respectively. The NOM mixture and BSA solutions exhibited a higher propensity for pore fouling relative to the alginate and humic acid test waters.
- The NOM mixture and BSA were more sensitive to changes in pressure and temperature, as determined by GLM and 3D surface plots, and exhibited higher fouling as temperature decreased and pressure increased.
- The normalization model presented was useful in estimating the MFI-UF values away from standard conditions for the different NOM fractions, which varied between 10% and 15% as pressure and temperature changed.
- The MFI-UF_{exp} values changed by >30% as pressure and temperature were varied, likely due to changes in fouling layer characteristics by cake compression and/or shrinkage.

Acknowledgment

The authors would like to acknowledge the Saudi Arabia Ministry of Education (MOE) and Natural Sciences and Engineering Research Council of Canada (NSERC) for helping fund this research.

References

[1] W. Gao, H. Liang, J. Ma, M. Han, Z.L. Chen, Z.S. Han, G.B. Li, Membrane fouling control in ultrafiltration technology for drinking water production: a review, Desalination, 272 (2011) 1–8.
[2] R. Peiris, M. Jaklewicz, Assessing the role of feed water constituents in irreversible membrane fouling of pilot-scale ultrafiltration drinking water treatment systems, Water Res., 47 (2013) 3364–3374.
[3] W.Q. Betancourt, J.B. Rose, Drinking water treatment processes for removal of Cryptosporidium and Giardia, Veter. Paras., 126 (2004) 219–234.
[4] W. Guo, H. Ngo, J. Li, A mini-review on membrane fouling, Bioresour. Technol., 122 (2012) 27–34.
[5] A. Zularisam, A. Ahmad, M. Sakinah, A. Ismail, T. Matsuura, Role of natural organic matter (NOM), colloidal particles, and solution chemistry on ultrafiltration performance, Sep. Purif. Technol., 78 (2011) 189–20.
[6] M. Zazouli, S. Nasseri, M. Ulbricht, Fouling effects of humic and alginic acids in nanofiltration and influence of solution composition, Desalination, 250 (2010) 688–692.
[7] K. Katsoufidou, D. Sioutopoulos, S. Yiantsios, A. Karabelas, UF membrane fouling by mixtures of humic acids and sodium alginate: fouling mechanisms and reversibility, Desalination, 264 (2010) 220–227.
[8] R. Nagel, Seawater desalination with polyamide hollow fiber modules at DROP, Desalination, 63 (1987) 225–246.
[9] J.C. Schippers, J. Verdouw, The modified fouling index: a method of determining the fouling characteristics of water, Desalination, 32 (1980) 137–148.
[10] S. Boerlage, M. Kennedy, M. Dickson, D. El-Hodali, J.C. Schippers, The modified fouling index using ultrafiltration membranes (MFI-UF): characterisation, filtration mechanisms and proposed reference membrane, J. Membr. Sci., 197 (2002) 1–21.
[11] S. Boerlage, M. Kennedy, Z. Tarawneh, R. Faber, J. Schippers, Development of the MFI-UF in constant flux filtration, Desalination, 16 (2004) 103–113.
[12] S. Rodriguez, G. Amy, J.C. Schippers, M. Kennedy, The Modified Fouling Index ultrafiltration constant flux for assessing particulate/colloidal fouling of RO systems, Desalination, 365 (2015) 79–91.
[13] S. Jeong, S. Vigneswaran, Practical use of standard pore blocking index as an indicator of biofouling potential in seawater desalination, Desalination, 365 (2015) 8–14.
[14] L.O. Villacorte, Y. Ekowati, H. Winters, G. Amy, J. Schippers, M.D. Kennedy, MF/UF rejection and fouling potential of algal organic matter from bloom-forming marine and freshwater algae, Desalination, 367 (2015) 1–10.
[15] A. Taheri, L.N. Sim, C. Haur, E. Alkhondi, A. Fane, The fouling potential of colloidal silica and humic acid and their mixtures, J. Membr. Sci., 433 (2013) 112–120.
[16] Y. Ju, I. Hong, S. Hong, Multiple MFI measurements for the evaluation of organic fouling in SWRO desalination, Desalination, 365 (2015) 136–143.
[17] S. Boerlage, M.D. Kennedy, M.P. Aniye, E. Abogrean, Z.S. Tarawneh, J.C. Schippers, The MFI-UF as a water quality test and monitor, J. Membr. Sci., 211 (2003) 271–289.
[18] J.C. Crittenden, R.R. Trussell, D.W. Hand, K.J. Howe, G. Tchobanoglous, Water Treatment: Principles and Design, 2nd ed., Montgomery Watson Harza, Ed., Wiley, New Jersey, 2005.
[19] M. Hashino, K. Hirami, M. Katagiri, T. Kubota, Effects of three natural organic matter types on cellulose acetate butyrate microfiltration membrane fouling, J. Membr. Sci., 379 (2011) 233–238.
[20] D. Jermann, W. Pronk, M. Boller, Mutual influences between natural organic matter and inorganic particles and their combined effect on ultrafiltration membrane fouling, Environ. Sci. Technol., 42 (2008) 9129–9136.
[21] M. Kitis, T. Karanfil, A. Wigton, J. Kilduff, Probing reactivity of dissolved organic matter for disinfection by products formation using XAD-8 resin adsorption and UF fractionation, Water Res., 36 (2002) 3834–3848.
[22] D.B. Mosqueda-Jimenez, Impact of Manufacturing Conditions of Poly Ethersulfone Membranes on Final Characteristics and Fouling Reduction, PhD Thesis, Department of Civil Engineering, University of Ottawa, Ottawa, ON, 2003.
[23] C. Ho, A. Zydney, A Combined pore blockage and cake filtration model for protein fouling during microfiltration, J. Colloid Interface Sci., 232 (2000) 389–399.
[24] ASTM International, Standard test method for modified fouling index (MFI-0.45) of Water, Designation (2015) D8002–15.
[25] S. Kertész, Z. László, Z.H. Horváth, C. Hodúr, Analysis of nanofiltration parameters of removal of an anionic detergent, Desalination, 221 (2008) 303–311.

Supplementary information

Table S1(a)
ANOVA and multiple comparisons (Tukey HSD) (95% confidence interval)

Operating pressure (bar)	MFI-UF_{HA} *p*-value (0.002)*	MFI-UF_{BSA} *p*-value (0.001)*	MFI-UF_{SA} *p*-value (0.008)*	MFI-UF_{Mix} *p*-value (0.001)*
1 vs. 2	0.010	0.001	0.036	0.005
1 vs. 3	0.001	0.002	0.007	0.001
2 vs. 3	0.010	0.001	0.046	0.004

**p*-value of all data set for each NOM model.

Table S1(b)
ANOVA and multiple comparisons (Tukey HSD) (95% confidence interval)

Water temperature (°C)	MFI-UF_{HA} *p*-value (0.001)*	MFI-UF_{BSA} *p*-value (0.002)*	MFI-UF_{SA} *p*-value (0.001)*	MFI-UF_{Mix} *p*-value (0.002)*
5 vs. 10	0.005	0.027	0.023	0.046
5 vs. 20	0.001	0.001	0.005	0.001
5 vs. 30	0.003	0.0003	0.001	0.002
5 vs. 35	0.002	0.002	0.001	0.001
10 vs. 20	0.042	0.012	0.031	0.009
10 vs. 30	0.007	0.003	0.004	0.002
10 vs. 35	0.006	0.001	0.004	0.001
20 vs. 30	0.030	0.036	0.041	0.037
20 vs. 35	0.044	0.041	0.035	0.040
30 vs. 35	0.042	0.038	0.050	0.045

**p*-value of all data set for each NOM model.

Table S1(c)
Regression coefficients for the predicted MFI-UF models

Model NOM	Regression coefficients		
	Unstandardized β_0*	Unstandardized (standardized) β_1*	Unstandardized (standardized) β_2*
Humic acid	1,588.858	2,058.965 (0.652)	−121.343 (−0.623)
Protein (BSA)	3,351.687	3,681.250 (0.721)	−201.537 (−0.691)
Sodium alginate	1,189.372	3,139.250 (0.755)	−140.453 (−0.609)
Mixture	2,598.917	3,537.500 (0.739)	−173.452 (−0.653)

*β_0: intercept; β_1: pressure effect; and β_2: temperature effect.